

Supporting Information for:

Iridium(III) complexes containing a *N*-heterocyclic carbene ligand: an experimental and theoretical study of structural, spectroscopic, electrochemical and electrogenerated chemiluminescence properties

Gregory J. Barbante,¹ Egan H. Doeven,¹ Paul S. Francis,¹ Bradley D. Stringer,² Conor F. Hogan,^{2*} Peyman R. Kheradmand,² David J. D. Wilson² and Peter J. Barnard^{2*}

*Authors for correspondence. Email: p.barnard@latrobe.edu.au and c.hogan@latrobe.edu.au

¹Centre for Chemistry and Biotechnology, School of Life and Environmental Sciences, Faculty of Science, Engineering and Built Environment, Deakin University, Geelong, Victoria 3216, Australia.

²Department of Chemistry and Physics, La Trobe Institute for Molecular Science, La Trobe University, Victoria 3086, Australia.

NMR spectroscopy

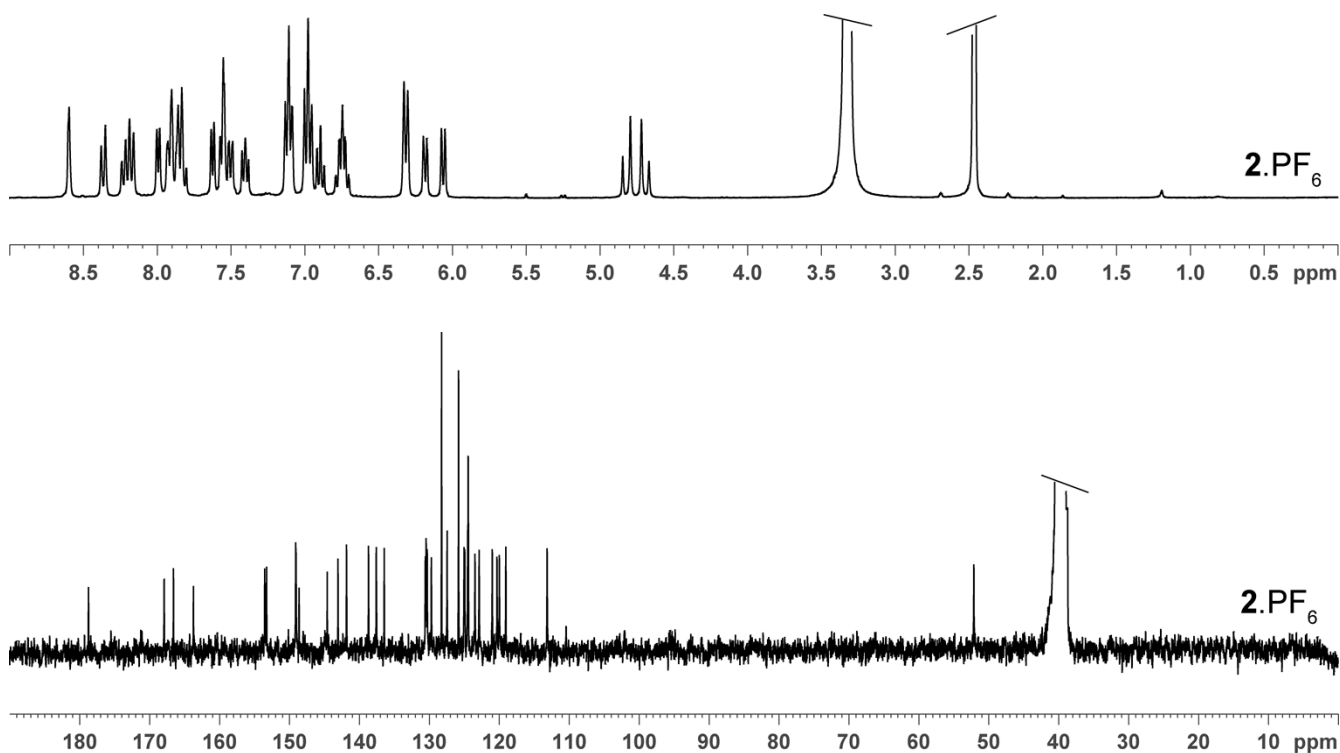


Figure S1. ¹H NMR spectra (upper) and ¹³C NMR spectra (lower) for the Ir(III) complex (a) 2.PF₆.

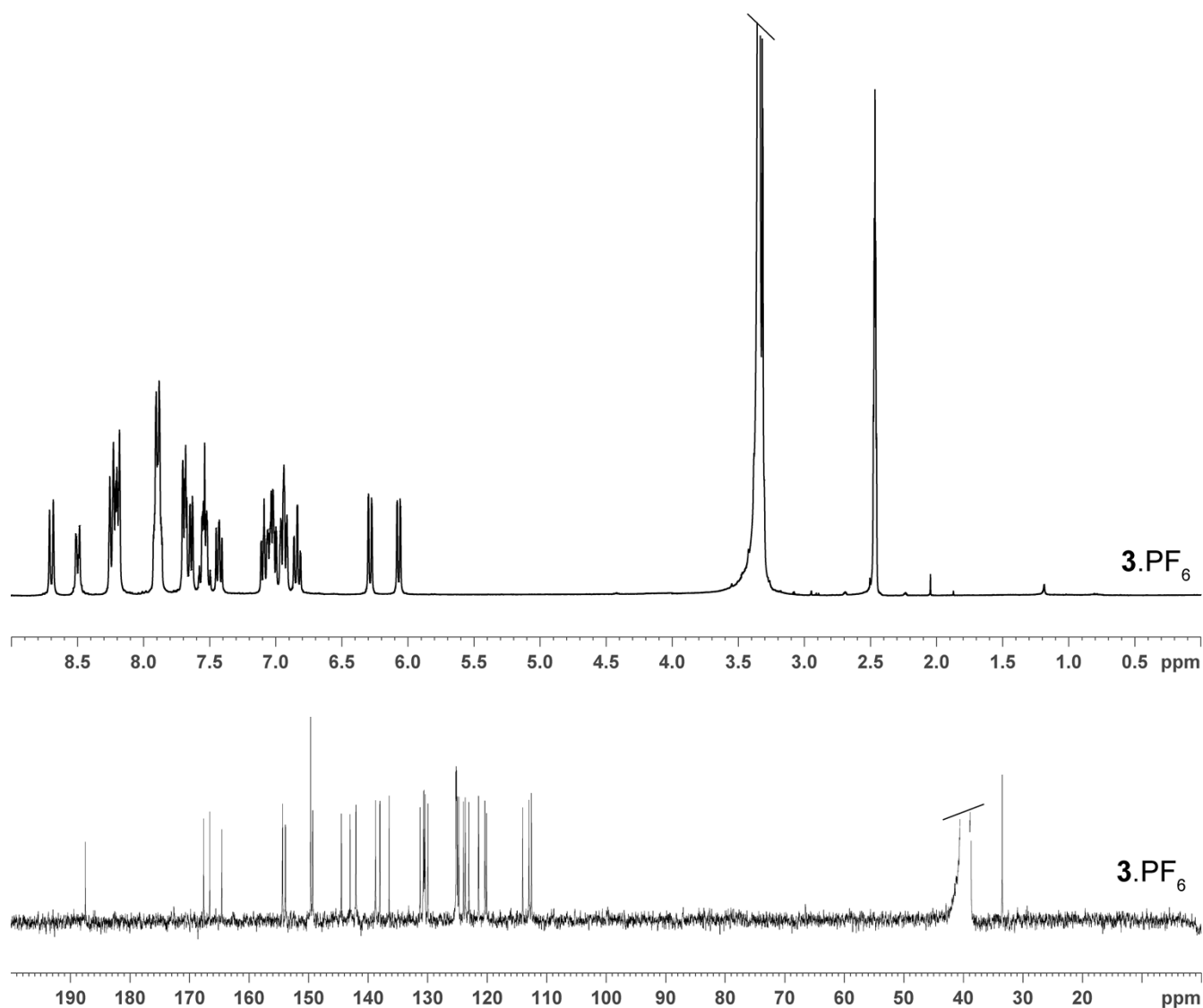


Figure S2. ^1H NMR spectra (upper) and ^{13}C NMR spectra (lower) for the Ir(III) complex (a) $3.\text{PF}_6$.

X-Ray Crystallography

Details:

$1.\text{PF}_6$: Solved in the orthorhombic space group $Pbca$ using direct methods. The asymmetric unit contains the title compound.

$3.\text{PF}_6$: Solved using Direct method in the monoclinic space group $P2_1/n$. The asymmetric unit contains the title compound and one co-crystallised methanol molecule. Disorder was identified in the position of the hydroxyl group of the methanol molecule, with the hydroxyl group occupying two crystallographically independent positions that could be located from the additional residual electron

density. Refinement of the site occupancy factors for the disordered atoms gave the value 0.46 and 0.34 respectively. There was no obvious hydrogen bond acceptor for the hydroxyl group and no hydrogen was placed on the oxygen atom of this molecule.

4.PF₆: Solved using Direct method in the monoclinic space group *P2₁/c*. The asymmetric unit contains the title compound. Disorder was observed in the phenyl ring of the benzyl substituent on the NHC ligand (C15 - C19), with these atoms are occupying two crystallographically independent positions that could be located from the additional residual electron density. AFIX constraints were applied to give the two disordered components of the phenyl ring a regular hexagonal shape and refinement of the site occupancy factors for the disordered atoms gave the value 0.75 and 0.25, respectively.

Theoretical Studies

Table S1. Fragment MO populations from Mulliken population analysis for **1⁺** (mPW1PW91/SDD,tzvp//mPW1PW91/SDD,6-31+G(d) with acetonitrile PCM-SCRF).

Orbital	MO composition (%)			
	Ir	ppy 1	ppy 2	carbene
LUMO+3	2	14	22	62
LUMO+2	3	74	18	6
LUMO+1	3	3	30	65
LUMO	4	21	48	28
HOMO	33	40	23	4
HOMO-1	16	28	47	9
HOMO-2	41	16	20	23
HOMO-3	26	32	35	7

Table S2. Fragment MO populations from Mulliken population analysis for **2⁺** (mPW1PW91/SDD,tzvp//mPW1PW91/SDD,6-31+G(d) with acetonitrile PCM-SCRF).

Orbital	MO composition (%)			
	Ir	ppy 1	ppy 2	carbene
LUMO+3	2	13	22	63
LUMO+2	3	74	17	6
LUMO+1	2	3	35	60
LUMO	4	21	43	33
HOMO	33	40	23	4
HOMO-1	12	29	52	6
HOMO-2	44	16	14	26
HOMO-3	24	32	37	8

Table S3. Fragment MO populations from Mulliken population analysis for 3^+ (mPW1PW91/SDD,tzvp//mPW1PW91/SDD,6-31+G(d) with acetonitrile PCM-SCRF).

Orbital	MO composition (%)			
	Ir	ppy 1	ppy 2	carbene
LUMO+3	3	11	22	64
LUMO+2	3	72	20	6
LUMO+1	3	3	18	76
LUMO	4	24	57	16
HOMO	32	41	23	5
HOMO-1	7	29	61	2
HOMO-2	43	18	6	33
HOMO-3	21	31	38	10

Table S4. Fragment MO populations from Mulliken population analysis for 4^+ (mPW1PW91/SDD,tzvp//mPW1PW91/SDD,6-31+G(d) with acetonitrile PCM-SCRF).

Orbital	MO composition (%)			
	Ir	ppy 1	ppy 2	carbene
LUMO+3	3	10	21	67
LUMO+2	3	68	26	3
LUMO+1	3	3	12	81
LUMO	4	27	57	13
HOMO	31	41	23	5
HOMO-1	7	30	59	3
HOMO-2	42	18	6	33
HOMO-3	17	31	40	12

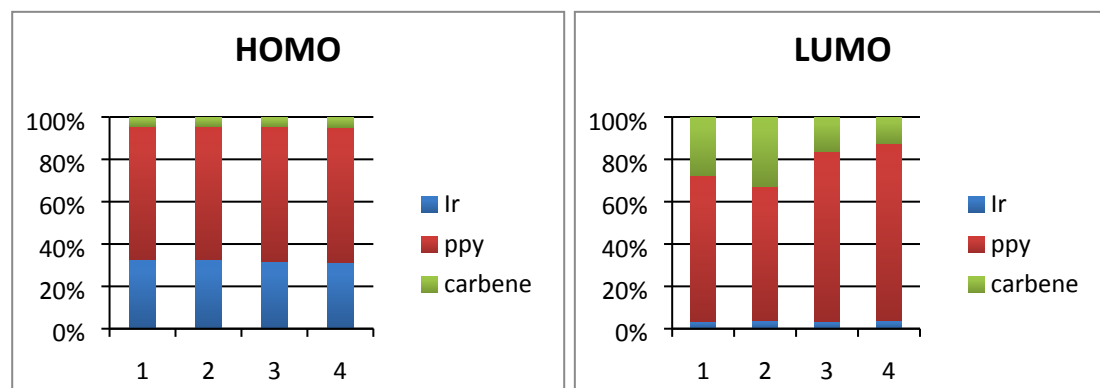


Figure S3. Fragment contributions to the HOMO and LUMO of complexes 1^{2+} - 4^{2+} (mPW1PW91/SDD,TZVP in acetonitrile PCM-SCRF). ppy = phenylpyridine, ligand = non-phenylpyridine ligand.

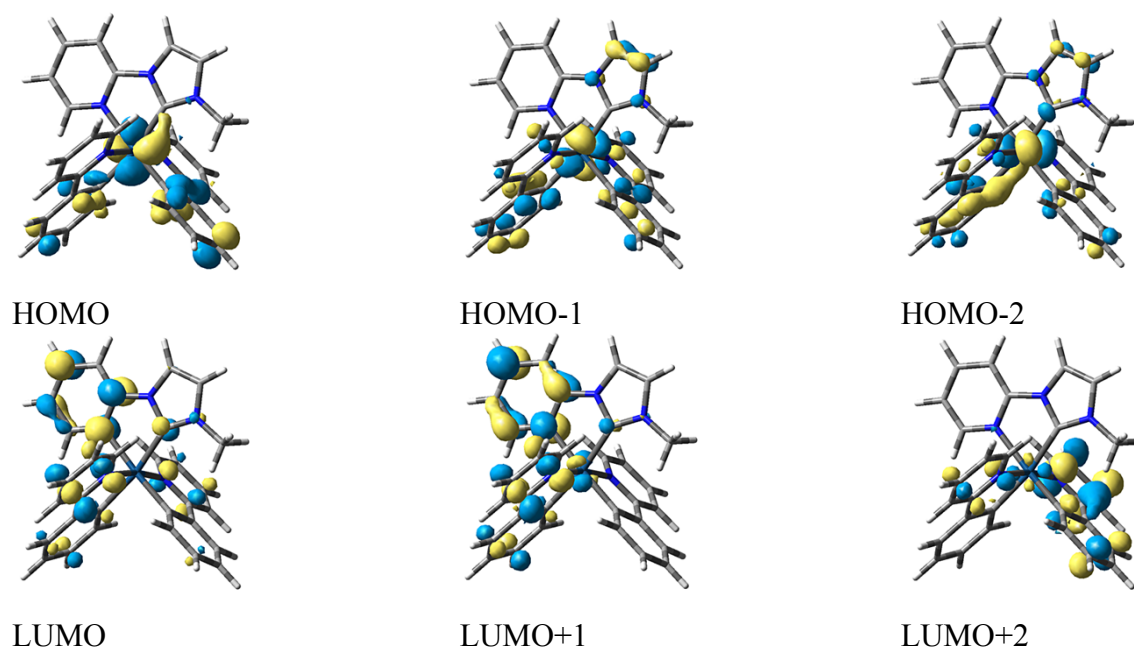


Figure S4. Frontier molecular orbitals of 1^+ (B3LYP/SDD,TZVP with acetonitrile PCM-SCRF at mPW1PW91/SDD,TZVP geometry).

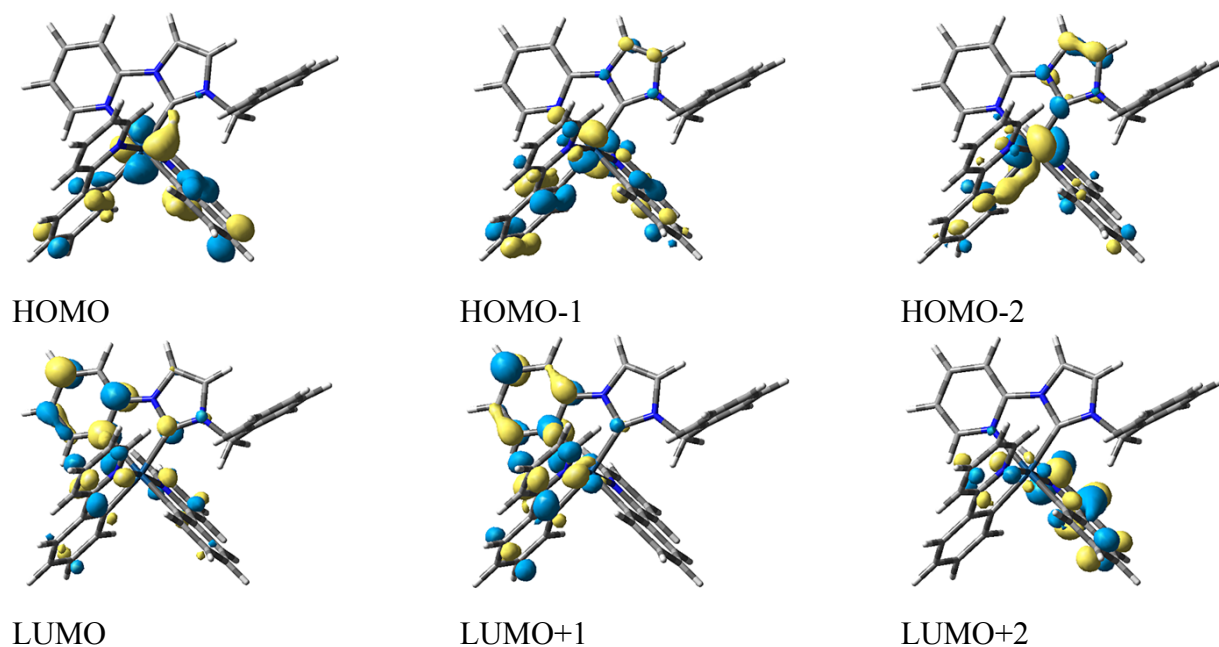


Figure S5. Frontier molecular orbitals of 2^+ (B3LYP/SDD,TZVP with acetonitrile PCM-SCRF at mPW1PW91/SDD,TZVP geometry).

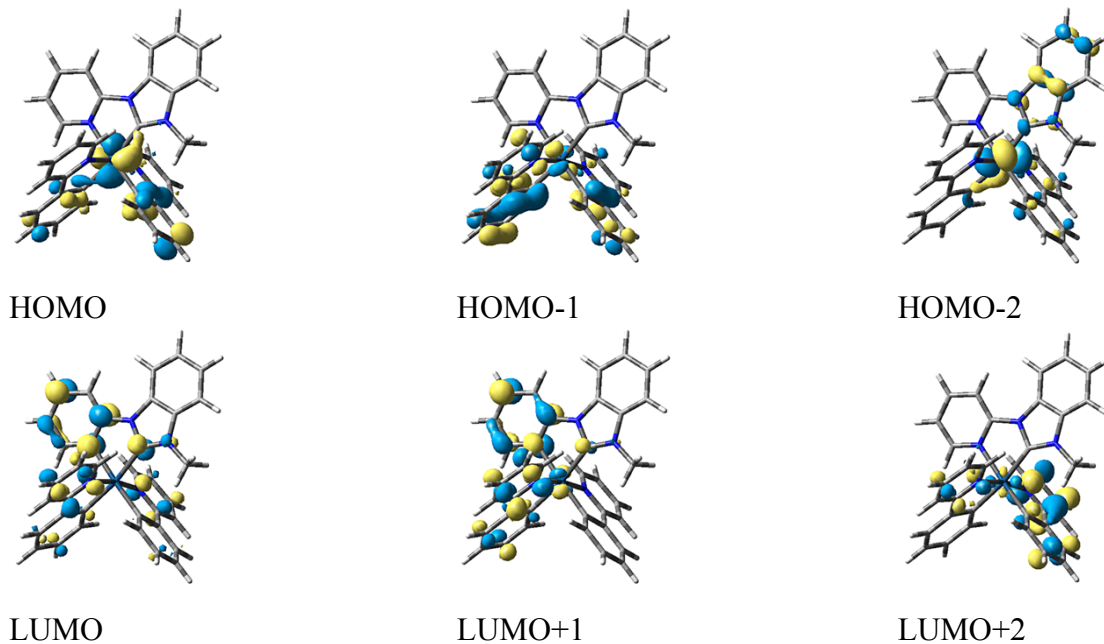


Figure S6. Frontier molecular orbitals of 3^+ (B3LYP/SDD,TZVP with acetonitrile PCM-SCRF at mPW1PW91/SDD,TZVP geometry).

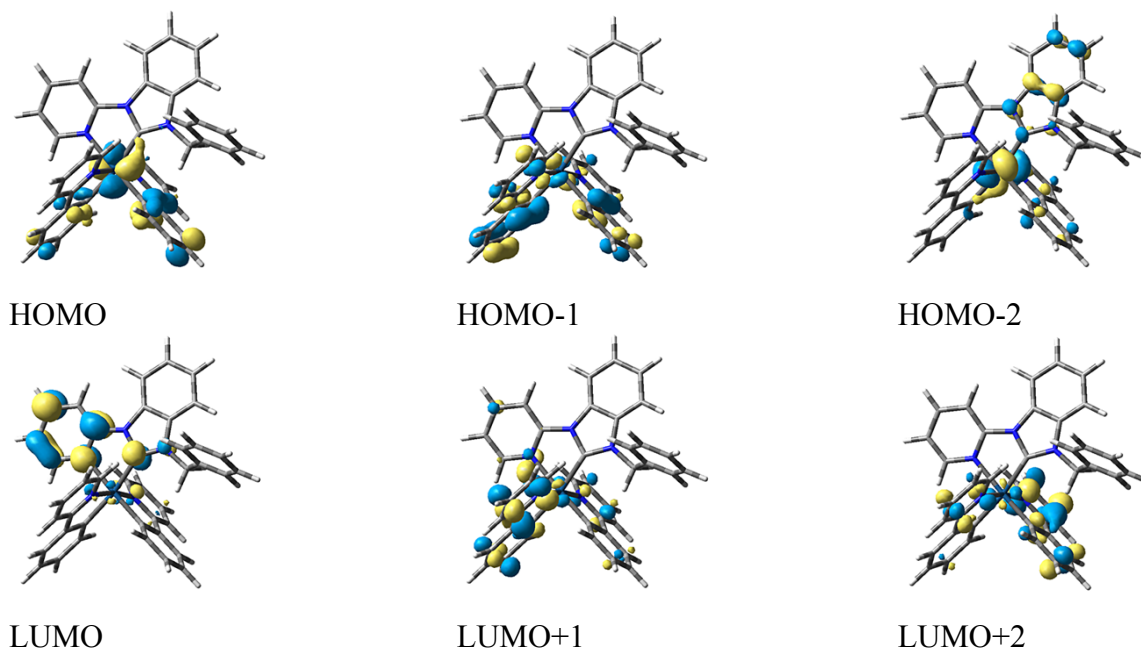


Figure S7. Frontier molecular orbitals of 4^+ (B3LYP/SDD,TZVP with acetonitrile PCM-SCRF at mPW1PW91/SDD,TZVP geometry).

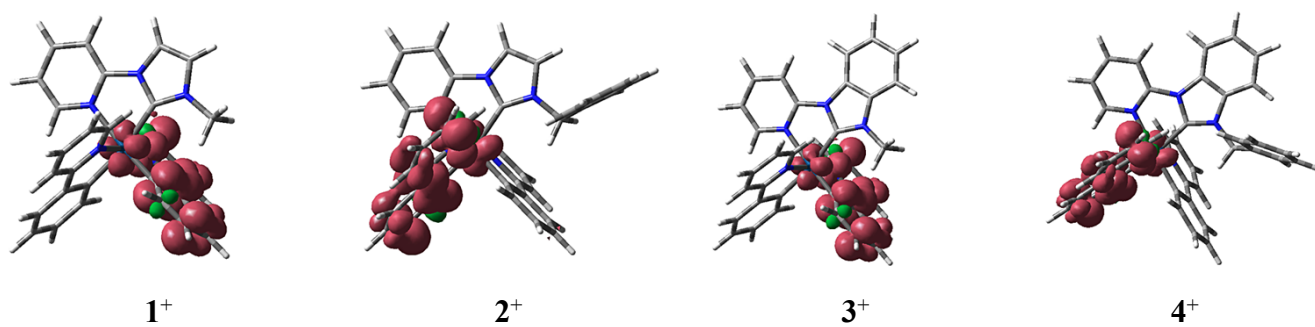


Figure S8. Triplet-state spin density for $1^+ - 4^+$ (B3LYP/SDD,TZVP with acetonitrile PCM-SCRF at mPW1PW91/SDD,TZVP geometry).

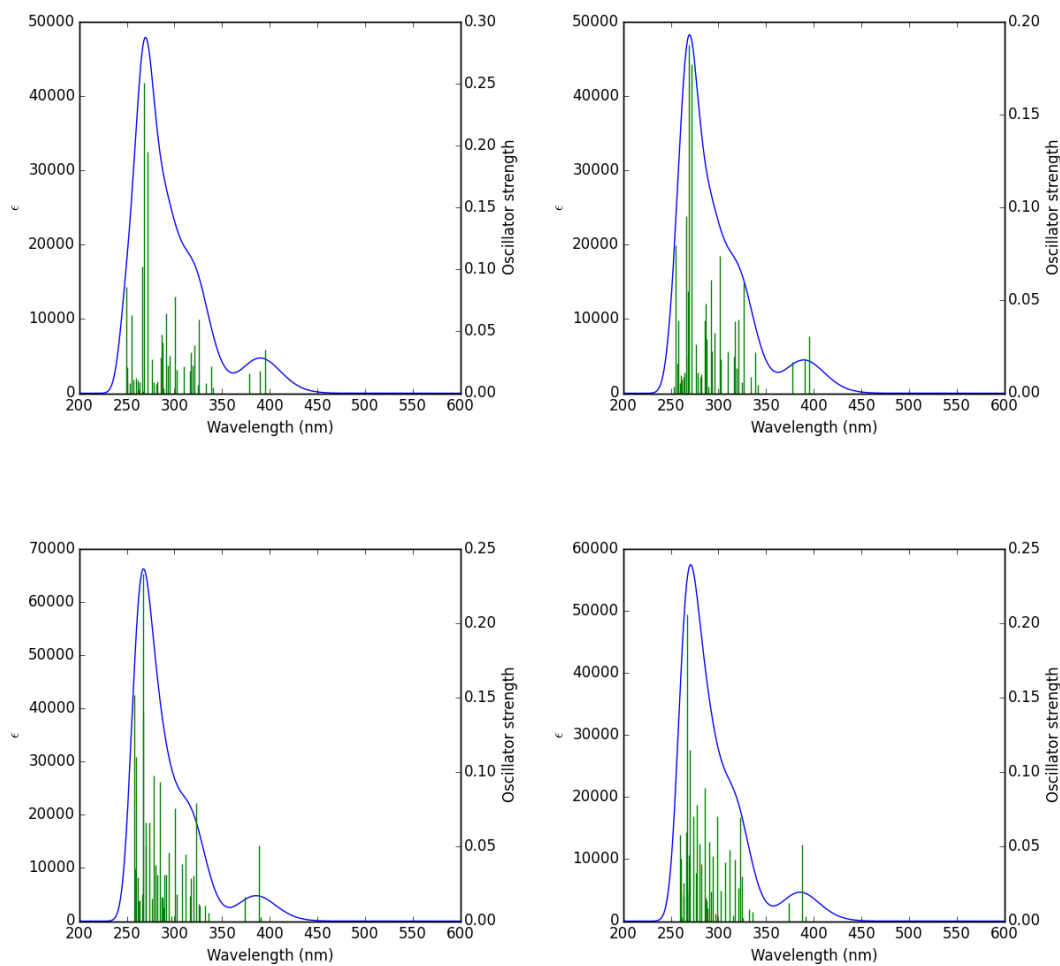


Figure S9. Calculated UV-Vis spectra for $1^+ - 4^+$ (B3LYP/def2-SVP//mPW1PW91/SDD,TZVP in acetonitrile PCM-SCRF). TD-DFT with 40 singlet and triplet states.

Table S5. Selected singlet states for complexes 1^+-4^+ calculated from TD-DFT (B3LYP/def2-SVP//mPW1PW91/SDD,6-31+G(D) with acetonitrile SCRf-PCM).

Compound	State	λ (nm)	f	Dominant excitation	Nature	Assignment
1^+	S1	395.2	0.036	H→L (96%)	$d_{\pi}(\text{Ir})+\pi_{\text{ppy}} \rightarrow \pi_{\text{ppy}}^* + \pi_{\text{carbene}}^*$	MLCT, LC, LLCT
	S2	390.1	0.018	H→L+1 (95%)	$d_{\pi}(\text{Ir})+\pi_{\text{ppy}} \rightarrow \pi_{\text{carbene}}^*$	MLCT, LLCT
	S3	378.1	0.016	H→L+2 (97%)	$d_{\pi}(\text{Ir})+\pi_{\text{ppy}} \rightarrow \pi_{\text{ppy}}^*$	MLCT, LC
	S27	271.9	0.195	H-1→L+5 (32%), H-4→L+2 (20%)	$d_{\pi}(\text{Ir})+\pi_{\text{ppy}} \rightarrow \pi_{\text{ppy}}^*$	MLCT, LC
	S28	268.3	0.251	H-2→L+5 (25%), H-1→L+5 (17%)	$d_{\pi}(\text{Ir})+\pi_{\text{ppy}} \rightarrow \pi_{\text{ppy}}^*$	MLCT
	S30	266.1	0.103	H-3→L+4 (51%)	$d_{\pi}(\text{Ir})+\pi_{\text{ppy}} \rightarrow \pi_{\text{carbene}}^*$	MLCT
	S36	255.1	0.063	H→L+6 (44%)	$d_{\pi}(\text{Ir})+\pi_{\text{ppy}} \rightarrow \pi_{\text{ppy}}^*$	MLCT
	S40	249.4	0.086	H-7→L (41%), H-4→L+5 (15%)	$d_{\pi}(\text{Ir})+\pi_{\text{ppy}} \rightarrow \pi_{\text{ppy}}^*$	MLCT
2^+	S1	395.5	0.031	H→L (97%)	$d_{\pi}(\text{Ir})+\pi_{\text{ppy}} \rightarrow \pi_{\text{ppy}}^* + \pi_{\text{carbene}}^*$	MLCT, LC, LLCT
	S2	390.4	0.019	H→L+1 (96%)	$d_{\pi}(\text{Ir})+\pi_{\text{ppy}} \rightarrow \pi_{\text{ppy}}^* + \pi_{\text{carbene}}^*$	MLCT, LC, LLCT
	S3	377.6	0.017	H→L+2 (97%)	$d_{\pi}(\text{Ir})+\pi_{\text{ppy}} \rightarrow \pi_{\text{ppy}}^*$	MLCT, LC
	S27	271.9	0.177	H-1→L+5 (25%), H-4→L+2 (19%)	$\pi_{\text{ppy}} \rightarrow \pi_{\text{ppy}}^*$	LC, LLCT
	S28	269.2	0.188	H→L+6 (23%), H-1→L+5 (18%), H-2→L+5 (17%)	$d_{\pi}(\text{Ir})+\pi_{\text{ppy}} \rightarrow \pi_{\text{carbene}}^*$	MLCT
	S31	266.4	0.095	H-3→L+4 (43%),	$d_{\pi}(\text{Ir})+\pi_{\text{ppy}} \rightarrow \pi_{\text{carbene}}^*$	MLCT
	S40	254.9	0.080	H→L+8 (39%)	$d_{\pi}(\text{Ir})+\pi_{\text{ppy}} \rightarrow \pi_{\text{carbene}}^*$	MLCT
3^+	S1	390.2	0.003	H→L (74%), H→L+1 (23%)	$d_{\pi}(\text{Ir})+\pi_{\text{ppy}} \rightarrow \pi_{\text{ppy}}^*$	MLCT, LC
	S2	388.9	0.051	H→L+1 (74%), H→L (24%)	$d_{\pi}(\text{Ir})+\pi_{\text{ppy}} \rightarrow \pi_{\text{carbene}}^*$	MLCT, LC, LLCT
	S3	374.1	0.016	H→L+2 (97%)	$d_{\pi}(\text{Ir})+\pi_{\text{ppy}} \rightarrow \pi_{\text{ppy}}^*$	MLCT, LC
	S8	323.2	0.080	H-1→L+5 (59%)	$\pi_{\text{ppy}} \rightarrow \pi_{\text{ppy}}^*$	LC
	S31	267.5	0.233	H-1→L+5 (25%), H-3→L+4 (19%)	$d_{\pi}(\text{Ir})+\pi_{\text{ppy}} \rightarrow \pi_{\text{ppy}}^* + \pi_{\text{carbene}}^*$	MLCT, LC, LLCT
	S32	266.8	0.140	H-3→L+4 (34%)	$d_{\pi}(\text{Ir})+\pi_{\text{ppy}} \rightarrow \pi_{\text{carbene}}^*$	MLCT
	S38	259.9	0.110	H-2→L+6 (27%), H-5→L+3 (25%)	$d_{\pi}(\text{Ir})+\pi_{\text{ppy}} \rightarrow \pi_{\text{carbene}}^*$	MLCT
	S40	258.2	0.152	H-5→L+3 (39%), H-2→L+6 (27%)	$d_{\pi}(\text{Ir})+\pi_{\text{ppy}} \rightarrow \pi_{\text{carbene}}^*$	MLCT
4^+	S1	391.3	0.003	H→L (62%), H→L+1 (35%)	$d_{\pi}(\text{Ir})+\pi_{\text{ppy}} \rightarrow \pi_{\text{ppy}}^* + \pi_{\text{carbene}}^*$	MLCT, LC
	S2	387.9	0.052	H→L+1 (62%), H→L (36%)	$d_{\pi}(\text{Ir})+\pi_{\text{ppy}} \rightarrow \pi_{\text{ppy}}^* + \pi_{\text{carbene}}^*$	MLCT, LC
	S3	373.6	0.012	H→L+2 (97%)	$\pi_{\text{ppy}} \rightarrow \pi_{\text{ppy}}^*$	LC
	S28	273.9	0.071	H-3→L+3 (41%), H-6→L (21%)	$d_{\pi}(\text{Ir})+\pi_{\text{ppy}} \rightarrow \pi_{\text{carbene}}^*$	LLCT
	S29	269.6	0.115	H-6→L+1 (39%), H-1→L+5 (19%)	$d_{\pi}(\text{Ir})+\pi_{\text{ppy}} \rightarrow \pi_{\text{carbene}}^*$	MLCT
	S32	267.3	0.206	H-6→L+1 (28%), H-1→L+5 (25%)	$d_{\pi}(\text{Ir})+\pi_{\text{ppy}} \rightarrow \pi_{\text{carbene}}^*$	MLCT

Table S6. Crystallographic data for Ir(III) complexes **1**·PF₆, **3**·PF₆, and **4**·PF₆

Identification code	1 ·PF ₆	3 ·PF ₆	4 ·PF ₆
Empirical formula	C ₃₁ H ₂₅ N ₅ F ₆ PIr	C ₃₆ H ₃₀ N ₅ F ₆ PIrO	C ₄₁ H ₃₁ N ₅ F ₆ PIr
Formula weight	804.73	885.82	930.88
Temperature/K	173.2	173.2	173.2
Crystal system	orthorhombic	monoclinic	monoclinic
Space group	Pbca	P21/n	P21/c
a/Å	10.9927(3)	13.818(3)	12.14380(14)
b/Å	16.3330(5)	13.881(3)	15.66023(14)
c/Å	31.7659(10)	17.586(4)	19.33573(19)
α/°	90	90	90
β/°	90	101.65(3)	101.3280(11)
γ/°	90	90	90
Volume/Å³	5703.4(3)	3303.5(12)	3605.53(6)
Z	8	4	4
ρ_{calc}/mg/mm³	1.874	1.781	1.715
m/mm⁻¹	4.81	4.163	3.817
F(000)	3136	1740	1832
Crystal size/mm³	0.08 × 0.04 × 0.03	0.06 × 0.05 × 0.05	0.1 × 0.1 × 0.04
Wavelength / Å	Mo-Kα 0.71073	Mo-Kα 0.71073	Mo-Kα 0.71073
θ range collected	4.98 to 52.04°	5.86 to 52.04°	4.94 to 52.04°
Index ranges	-9 ≤ h ≤ 13, -20 ≤ k ≤ 19, -39 ≤ l ≤ 37	-16 ≤ h ≤ 17, -17 ≤ k ≤ 17, -15 ≤ l ≤ 21	-14 ≤ h ≤ 14, -19 ≤ k ≤ 19, -23 ≤ l ≤ 23
Reflections collected	21889	24187	61518
Independent reflections	5615[R(int) = 0.0476]	6505[R(int) = 0.0258]	7102[R(int) = 0.0328]
Data/restraints/parameters	5615/0/398	6505/0/456	7102/18/503
Goodness-of-fit on F₂	1.04	1.095	1.079
Final R indexes [I > 2σ(I)]	R ₁ = 0.0365, wR ₂ = 0.0614	R ₁ = 0.0320, wR ₂ = 0.0703	R ₁ = 0.0189, wR ₂ = 0.0422
Final R indexes [all data]	R ₁ = 0.0647, wR ₂ = 0.0707	R ₁ = 0.0378, wR ₂ = 0.0728	R ₁ = 0.0224, wR ₂ = 0.0438
Largest diff. peak/hole/e Å⁻³	1.03/-0.86	2.91/-1.21	0.72/-0.41

Table S7 Absorbance data for Ir(III) complexes **1-4** in CH₃CN at room temperature.

Complex	λ / nm	ϵ / M ⁻¹ cm ⁻¹	
1	218	51930	sh
	255	54640	
	266	51440	
	308	21320	sh
	379	7110	
2	219	53640	sh
	254	49150	
	266	46570	
	310	18480	sh
	378	5980	
3	250	65950	
	268	61950	
	285	45310	sh
	316	22510	sh
	376	8050	
4	251	65060	
	268	62130	
	285	46760	sh
	317	21450	sh
	375	6650	